Journal of Applied Polymer Science

Rheological Assessment of Variable Molecular Chain Structures of Linear Low-Density Polyethylene Under Reactive Modification

Mahdi Golriz, Hossein Ali Khonakdar, Jalil Morshedian
Iran Polymer and Petrochemical Institute, P.O. Box 14965-115, Tehran, Iran
Correspondence to: H. A. Khonakdar (E-mail: hakhonakdar@gmail.com or h.khonakdar@ippi.ac.ir)

ABSTRACT: The aim of this study was to investigate how changes in the molecular structure of linear low-density polyethylene (LLDPE) during peroxide modification can be detected by a simple rheological method. For this purpose, a commercial-grade LLDPE (Exxon Mobile LL4004EL) was reacted with different doses of dicumyl peroxide (DCP). The samples were analyzed by size exclusion chromatography coupled with a light-scattering detector. With increasing DCP dose, at a roughly constant molar mass, an increasing number of long-chain branches were found. The dynamic shear oscillatory measurements showed a deviation of the phase angle–complex shear modulus curve from that of the linear LLDPE, which was attributed to the presence of long-chain branching. By the use of a simple rheological method that used melt rheology, transformations in the molecular architecture induced on the original LLDPE during the early stages of reactive modification were indicated. Reasonable and consistent estimates of the degree of long-chain branching (x) and the volume fraction of the various molecular species produced in the peroxide modification of LLDPE were obtained. Various three-dimensional plots were constructed to exhibit the correlation between the process parameters and x. © 2013 Wiley Periodicals, Inc. J. Appl. Polym. Sci. **2014**, *131*, 39617.

KEYWORDS: functionalization of polymers; polyolefins; rheology

Received 27 January 2013; accepted 3 June 2013
DOI: 10.1002/app.39617

INTRODUCTION

The flow behavior of macromolecular liquids is highly sensitive to the large-scale molecular structure. Linear polymers of the same species differ from one another in only one large-scale feature, the chain length or molecular weight. The viscoelastic parameters associated with flow depend systematically on the molecular weight. When the molecules are branched, the behavior varies with the number, location, and length of the branches. Some quite striking differences from linear polymer behavior are found, especially when entanglement interactions are important.[1] It is well known that a very low level of long-chain branching (LCB) has a significant effect on the specific processability of polymers, such as their extensibility, melt strength, and drawability.[2]

The determination of the LCB of polymers is essential to understanding their rheology and optimizing their processing behavior.[1,3] The only direct method for detecting long-chain branches in LCB polyethylenes (PEs) is NMR. This method, however, is very much limited in the case of low contents of long-chain branches, as very long measurement times are needed to detect low LCB contents.[4–6] Another problem is that NMR is unable to differentiate between side chains larger than six carbon atoms in length. The second technique is size exclusion chromatography (SEC) with coupled multiangle laser light scattering (MALLS), which is based on a comparison of the hydrodynamic radius[7–9] and is evaluated by the Zimm–Stockmayer method.[10]

This method, however, has been proven to not be optimal for finding low amounts of long-chain branches, too. LCB has its most significant effect on the polymer melt dynamics. Consequently, many authors have tried to exploit this rheological effect to characterize LCB.[11–19]

LCB can be incorporated directly during the synthesis, as is the case for traditional radically polymerized low-density PE and modern metallocene-catalyzed qualities. Another approach is the introduction of LCB by the light crosslinking (modification) of linear polyolefins in a postreactor reaction.[20] The main purpose of postreactor modification is to optimize the ease in plastic processing, to enhance the polarity, and to satisfy specific applications. Economic reasons are also taken into account.[21,22] Modification is normally done with peroxides, high-energy radiation, or vinyl silanes. In this study, modification with dicumyl peroxide (DCP) was used to introduce LCB in a linear low-density polyethylene (LLDPE). In the case of the random branching that occurs in free-radical polymerization, the structure can become enormously complicated, and it is impossible to draw any definitive conclusions from the rheological data on

branched polymers unless something is known about the type of branching structure involved. Random branching always leads to a broad distribution of structures; this makes it difficult to distinguish between the effects of branching and the polydispersity.

Many investigations have been accrued and different rheological methods have been proposed for detecting LCB in LCB PEs. Thermorheological complexity based on the failure of the time–temperature superposition principle has been proposed as an effective method to determine LCB existence.[23–26] Wood-Adams and Dealy[4,27] have shown how it is possible, in principle, to prescribe the molecular weight distribution (MWD) of a linear polymer that would have the same complex viscosity as any given branched polymer.

Another method often applied is the comparison of the dependence of the zero-shear-rate viscosity (η_0) on the weight-average molecular weight (M_w) of branched materials with that of the linear ones.[28–32] On the basis of this method, when the modification is of limited extent and does not progress much above the insertion of a single branching point per molecule on average, Tsenoglou and Gotsis,[31] proposed a simple rheological method for estimating the degree of long-chain branching (x; fraction of branched chains or, equivalently, the average number of branches per chain) of a polymer melt undergoing the early stages of a crosslink-inducing reactive modification. Their method applies to the LCB characterization of the relatively simple case of polypropylene (PP), where the modifier action introduces trifunctional branching and leaves the M_w roughly constant. They verified the accuracy of their method by comparing its predictions against the characterization results of a sophisticated analytical scheme involving high-temperature SEC with online light scattering, refractive index (RI) measurement, and intrinsic viscosity measurements of the effluent. Tsenoglou et al.[32] extended the method developed earlier for the simple case of PP modification via the addition of trifunctional chain-extending/branch-inducing agents[31] to tetrafunctional agents used for the modification of a linear poly(ethylene terephthalate).

The free-radical modification mechanism for PEs implied the formation of a random branch structure consisting of trifunctional and tetrafunctional vertices at the early stages of a crosslink-inducing reactive modification.[33–36] In this article, the term *crosslinking* is reserved for tetrafunctional (H-type) LCB resulting from a linkage between two macroradical backbones, and *end linking* is the trifunctional (T-type) LCB produced when a terminal group of a molecule forms a covalent bond with the backbone of another molecule. In fact, an originally linear chain is partially transformed via free-radical reaction into a star–linear mixture, in which star polymers have two different functionalities (fs = 3 and 4). The modulation of rheological modeling with a chemical modification mechanism representing a specific modifying agent results in simple and effective ways of monitoring the evolving molecular architecture of an initially linear polymer in the early stage of modification. The objective of this study was to extend the Tsenoglou and Gotsis approach to a case more complex than that of PP modification, where an originally linear LLDPE chain was partially transformed via peroxide modification into star polymers of two different fs (fs = 3 and 4).

Table I. k_d, Half-Life Time, and Estimated Number of Decompositions at 170, 185, and 200°C

Temperature (°C)	k_d (s^{-1})	Half-life time (s)	Estimated number of decompositions during mixing for different times		
			3 min	7.5 min	12 min
170	9.6×10^{-3}	72	2	6	10
185	3.8×10^{-2}	18	10	24	39
200	1.3×10^{-1}	5	35	87	139

EXPERIMENTAL

Materials

A commercial LLDPE (LL4004EL), with a melt flow index of 3.6 g/10 min (190°C,2.16 kg) and a density of 0.924 g/cm^3 (20°C), was obtained from ExxonMobil Chemical. The average molecular weight of this grade of LLDPE was about 95,000 g/mol. DCP (molecular weight = 270.37 g/mol) and xylene (a mixture of *o*-, *m*-, and *p*-xylene and whose boiling point was about 140°C and whose density was 0.87 g/cm^3 at 20°C) were chemically pure and were purchased from Aldrich Chemical Co. The decomposition rate constant of DCP (k_d), the half-life time, and the estimated number of decomposition steps at 170, 185, and 200°C as provided by the suppler are summarized in Table I.

Modification Procedure

Table II shows the preparation conditions of the peroxide-modified LLDPE at various residence times and temperatures. Samples with various peroxide concentrations (200, 700, and 1200 ppm) were prepared via melt compounding inside a DACA twin-screw microcompounder (DACA Instruments, Goleta, A) with a screw speed of 100 rpm and temperatures of 170, 185, and 200°C with various residence times, as shown in Table II. Sample preparation was based on a response surface methodology.

Gel Analysis

The most modified samples were examined for gel content according to ASTM 2765. According to this standard, the extraction in boiling xylene is the basis of all the analyses. The results revealed zero gel content; this indicated that the gel content of all of the peroxide-modified samples was negligible.

SEC

The molar masses, MWDs, radii of gyration, and branching parameters were obtained from measurements by high-temperature SEC coupled with a MALLS detector and an RI detector. The polymer molecules were fractionated by SEC by their hydrodynamic volume, which depended on the density in the dissolved state, molar mass, and LCB. Therefore, conventional SEC with linear polymer standards for the calibration is not suitable for investigations of the molar mass of branched polymer structures because of the fact that the calculated molar mass averages would be lower than the true values.[37] By

Table II. Preparation Conditions for the Peroxide-Modified LLDPEs with Various Residence Times and Temperatures

Sample code: ppm/°C/min	Peroxide concentration (ppm)	Mixing temperature (°C)	Mixing time (min)	Mixer speed (rpm)
P200/170/7.5	200	170	7.5	100
P200/185/3	200	185	3	100
P200/185/12	200	185	12	100
P200/200/7.5	200	200	7.5	100
P700/170/3	700	170	3	100
P700/170/12	700	170	12	100
P700/185/7.5	700	185	7.5	100
P700/200/3	700	200	3	100
P700/200/12	700	200	12	100
P1200/170/7.5	1200	170	7.5	100
P1200/185/3	1200	185	3	100
P1200/185/12	1200	185	12	100
P1200/200/7.5	1200	200	7.5	100
P0/170/3	0	170	3	100
P0/170/7.5	0	170	7.5	100
P0/170/12	0	170	12	100
P0/185/3	0	185	3	100
P0/185/7.5	0	185	7.5	100
P0/185/12	0	185	12	100
P0/200/3	0	200	3	100
P0/200/7.5	0	200	7.5	100
P0/200/12	0	200	12	100
P0/0/0 or virgin LLDPE	0	—	—	—

coupling SEC with MALLS, we could directly determine the absolute molar mass (M_{LS}) and radius of gyration of every fraction. Therefore, no calibration with a standard was done for the calculation of the molar masses because of the presence of branching. The ratio of the mean-square radius of gyration of a branched polymer ($\langle S^2\rangle_{br}$) to the radius of gyration for a linear polymer ($\langle S^2\rangle_{lin}$) is the so-called Zimm–Stockmayer branching parameter (g):[10]

$$g=\frac{\langle S^2\rangle_{br}}{\langle S^2\rangle_{lin}} \quad (1)$$

For the peroxide-modified LLDPE, a trifunctional and tetrafunctional randomly branched architecture could be assumed because the formation of branching points with a higher f was not probable for statistical reasons.[38] For such a trifunctional, randomly branched polymer, g can be related to branching by

$$g=\left[\left(1+\frac{m}{7}\right)^{0.5}+\frac{4m}{9\pi}\right]^{-0.5} \quad (2)$$

For a tetrafunctional, randomly branched polymer, g can be related to branching by

$$g=\left[\left(1+\frac{m}{6}\right)^{0.5}+\frac{4m}{9\pi}\right]^{-0.5} \quad (3)$$

where m is the number of long-chain branches along the molecule.[10] From that, the number of long-chain branches per 1000 monomer units (λ) was determined as

$$\lambda=\frac{m}{M}\times 1000\times M_M \quad (4)$$

where M_M is the molar mass of the monomer unit and M is the molar mass of the branched polymer. The SEC experiments were carried out with a PL-GPC 220 apparatus (Polymer Laboratories) at 150°C coupled with a MALLS detector (Helleos II, Wyatt Technology Corp.) and an RI detector. The column set consisted of two columns (PL Mixed-B-LS, Polymer Laboratories). The eluent was 1,2,4-trichlorobenzene (Merck) stabilized with 0.02 wt % 2,6-di-*tert*-butyl-*p*-cresol (BHT) as a solvent. The software used for data processing and calculation of the LCB number was Astra 5 (Wyatt Technology Corp.). The *dn*/*dc* value of PP was 0.104 mL/g. With this value, the M_{LS}'s were determined.

Rheometry

The melt rheological properties of the samples were determined with an ARES rheometer (Rheometric Scientific). The measurements were performed in the dynamic mode with 25-mm parallel-plate geometry with gap settings according to the disk thickness under a liquid nitrogen atmosphere. The strain amplitude was kept at 10% in the whole frequency range; this was determined to be in the linear viscoelastic range by strain sweeps for the compositions presented in this article.

The linear viscoelastic properties of the samples were measured at different temperatures (160, 180, and 200°C); the frequency was varied between 100 and 0.03 rad/s. Because of the inherent properties of the reactive processes, the probability of the existence of residual peroxide in the samples and its effects on the linear viscoelastic properties were checked by a frequency sweep test from 100 to 0.03 rad/s and back again. In this study, the η_0 data were determined on the basis of the Maxwell model with built-in rheometer software.

RESULTS AND DISCUSSION

Molecular Characterization

Changes in Molecular Mass Distributions. The MWDs of the samples modified with 0-, 200-, 700-, and 1200-ppm peroxide prepared under different processing conditions are plotted in Figure 1. The changes in the average molecular weight and MWD induced by peroxide modification under various conditions were small. Also, there were no indications of the formation of low-molecular-weight fractions due to chain scission. This implied that the degradation process was not predominant in the high-molecular-mass area of the polymer.

m versus M_{LS} calculated according to eqs. (2)–(4) for samples modified with different levels of peroxide are summarized in Table III. It was clear that the development of LCB was more pronounced at lower molecular weights (i.e., 70,000 g/mol) than at high molecular weights (i.e., 300,000 g/mol). This was due to an easing of peroxide diffusion into the system with shorter chains.

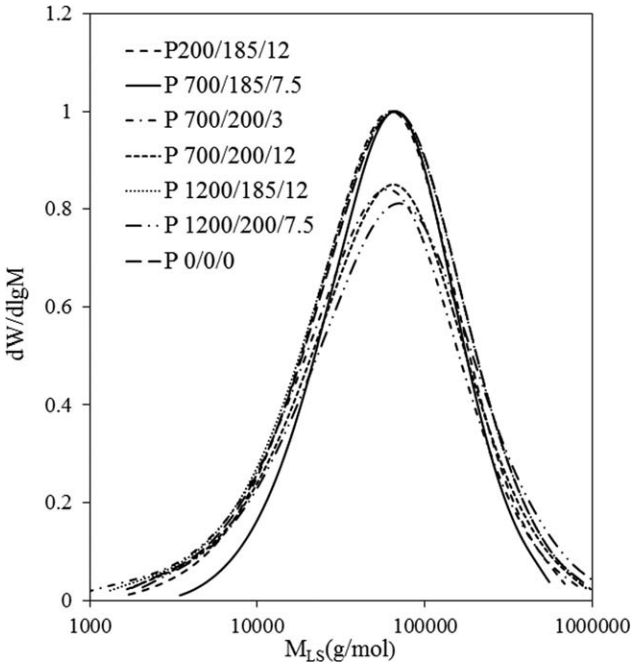

Figure 1. MWDs (dW/d log M) for the initial LLDPE (P0/0/0) and DCP-modified LLDPEs.

Because M_w and MWD did not change with peroxide modification, to examine the influence of the peroxide modification on x, a double-logarithmic plot of η_0 as a function of M_w was constructed on the basis of $\eta_0 = K$, the $M_w{}^{\alpha}$ equation for the original LLDPE and the peroxide-modified LLDPE samples. An exponential dependence of η_0 on the molar mass is known from the literature for starlike branched polymers; it exceeds the power law and is valid for linear polymers at high molar masses.[28] The results are presented in Figure 2. We observed that η_0 of LLDPE came to lie on the line valid for linear PEs. The η_0 values of the LCB LLDPE materials were above the reference line of linear materials. Because the molecular weight and MWD did not significantly change, this deviation could be attributed to structural changes induced by branching.

Table III. m versus M_{LS} as Determined by Light Scattering for Samples Modified with Different Levels of Peroxide

	LCBs per molecule at M_{LS}	
Sample code: ppm/°C/min	≈70,000	≈300,000
P200/170/7.5	1.53	0.30
P200/185/3	1.17	0.20
P200/185/12	0.94	0.54
P200/200/7.5	0.46	0.09
P700/170/3	0.59	0.02
P700/170/12	0.84	0.03
P700/185/7.5	0.47	0.16
P700/200/3	0.96	0.83
P700/200/12	0.64	0.32
P1200/170/7.5	0.65	0.01
P1200/185/3	0.28	0.00
P1200/185/12	0.55	0.13
P1200/200/7.5	0.58	0.11
P0/200/3	0.28	0.00
P0/200/7.5	0.27	0.00
P0/200/12	0.75	0.01

Rheological Measurements

Rheological Characterization of the Thermal Stability. Because of inherent property of reactive processes and the probability of the existence of residual peroxide in the samples, it was necessary to confirm that the polymer structure did not change during the measurements. To examine the stability and repeatability of the melt at test temperatures, the critical sample P700/170/3 from Table II was selected. Sample P700/170/3 had the lowest mixing temperature (lowest number of peroxide decomposition) and the lowest mixing time among all of samples. In a peroxide modification process, there are several competitive reactions, such as transfer, scission, and termination reactions. The extent of these reactions does not depend on the temperature only. Other parameters, such as the peroxide concentration, peroxide half-life time at the processing temperature, and the remaining peroxide, are also involved. According to Table I, the P700/170/3 sample selected for the thermal stability analysis had the highest peroxide half-life time (i.e., the lowest number of peroxide decompositions) because of the low processing time and temperature, and therefore, it most likely contained the highest amount of unreacted peroxide.

In this sample, the storage modulus, loss modulus, and complex viscosity were measured as a function of the frequency from 100 to 0.03 rad/s and back again (Figure 3). From the observed superposition of the results obtained during the high-to-low and low-to-high frequency sweeps, it was clearly evident that the sample did not undergo any structural changes during the rheological measurement. Although the time sweep could also be used for this purpose because each frequency sweep took

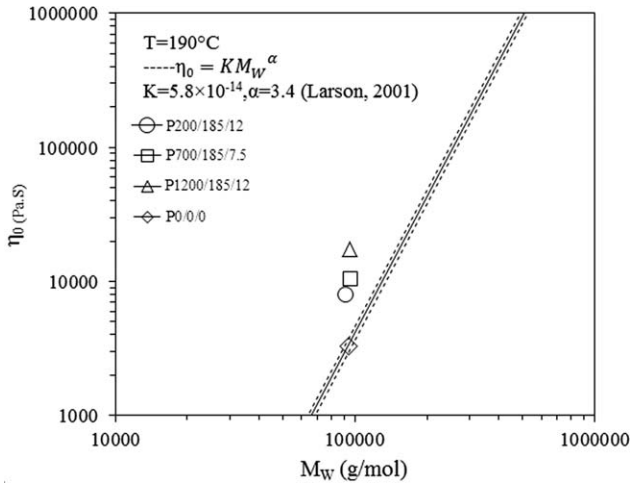

Figure 2. η_0–M_w plot for the samples with induced long-chain branches and the linear sample. The dashed line represents a ±5% uncertainty in M_w (T = temperature).

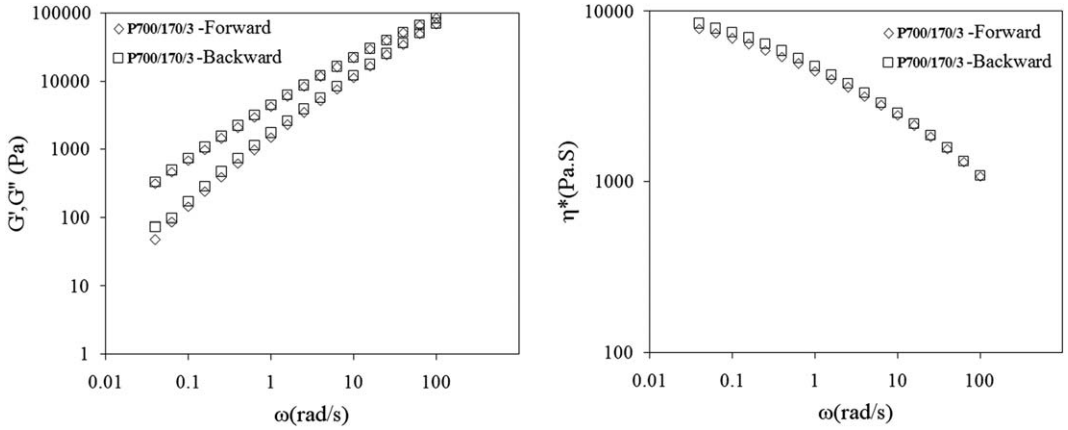

Figure 3. Determination of the thermal stability by measurement of the storage modulus (G'), loss modulus (G''), and complex viscosity (η^*) as a function of the frequency (ω) from 100 to 0.03 rad/s and back again obtained at 180°C.[39]

about 20 minutes, it is a common practice for showing the structural stability of samples during rheological tests.

Oscillatory Shear Flow Measurements. The dynamic shear oscillatory measurements were performed at 160, 180, and 200°C.

The results from these measurements are presented in different forms in Figures 4–6. Sample preparation was done on the basis of a response surface design methodology. So, the rheological parameters, such as η_0, loss angle, elastic modulus, and loss modulus, were the response surface parameters. To separate the effect of the processing parameters on the rheological properties of the samples, the complex viscosity versus the peroxide concentration, processing time, and processing temperature obtained at 180°C are shown in Figure 4(a–c), respectively. A

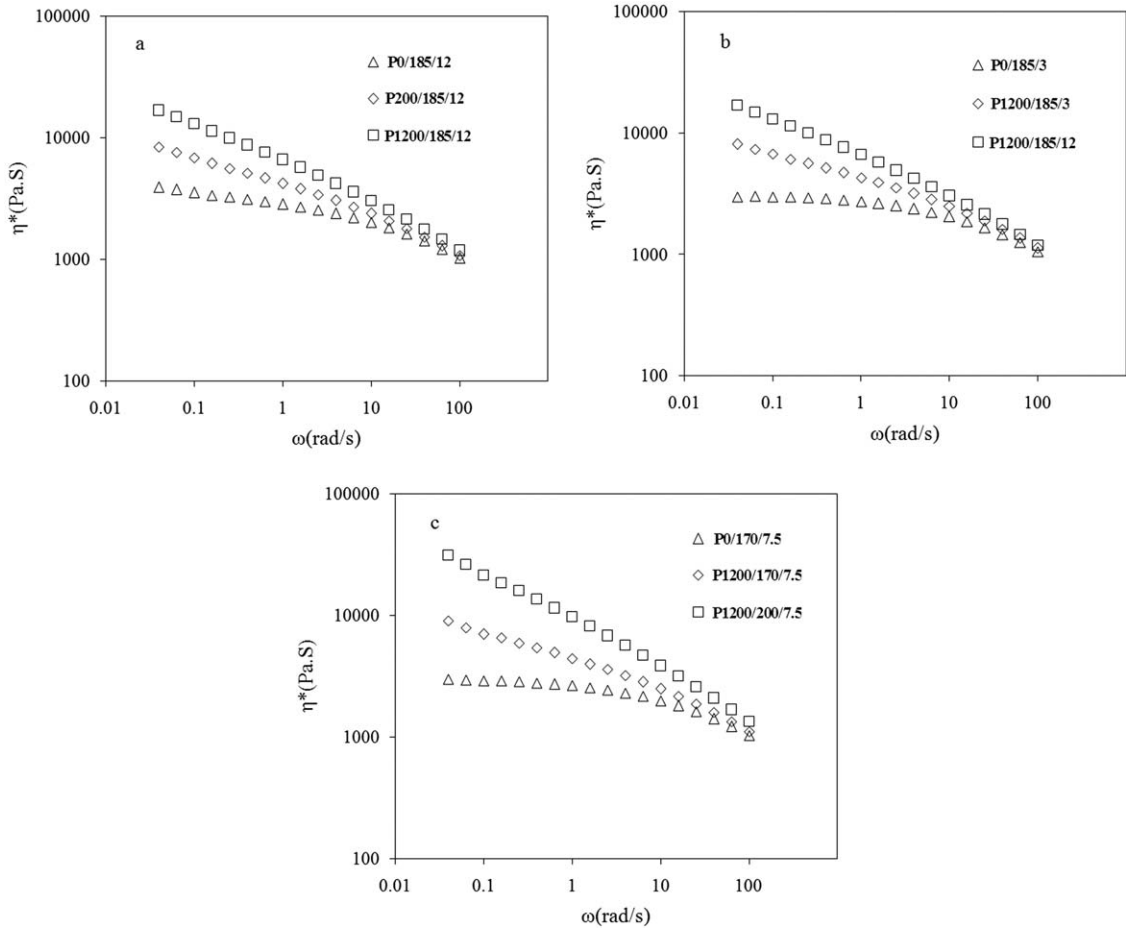

Figure 4. Complex viscosity versus the processing conditions. Effects of the (a) peroxide concentration, (b) processing time, and (c) processing temperature obtained at 180°C.

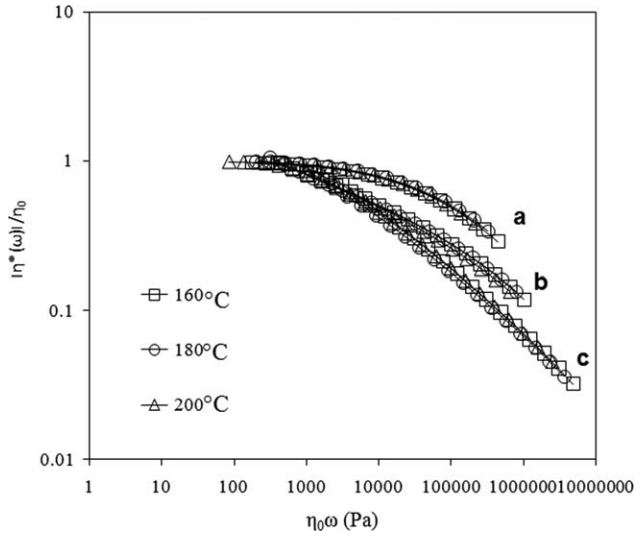

Figure 5. Reduced plots at 160, 180, and 200°C for (a) virgin LLDPE (P0/0/0), (b) P200/185/12, and (c) P1200/200/7.5.

clear viscosity enhancement at a low deformation rate with increasing peroxide concentration was evident. The complex viscosity is shown as a reduced plot (Figure 5) to assess the shear-thinning behavior, which is an important issue from a practical point of view. The shear-thinning behavior was found to be changed for the peroxide-modified samples. For example, samples P200/185/12 and P1200/200/7.5 showed a clear change in comparison with the unmodified linear sample (P0/0/0). As the polydispersity (M_w/number-average molecular weight) of the LLDPE investigated did not change very much with the peroxide modification, we concluded that the introduced branching had no pronounced effect on the shear-thinning behavior. Recently, plots of the phase angle (δ) versus the complex shear modulus [$|G^*(\omega)|$] have frequently been used to obtain insight into LCB.[40,41] Such plots were constructed for the modified samples, and the results are presented in Figure 6.

In the medium range of $|G^*(\omega)|$ between the rubbery plateau region and the Newtonian region, a deviation of δ beneath the curve of the linear LLDPE was observed for the samples modified with 200-ppm peroxide and higher. A shift of δ toward small values at a fixed $|G^*(\omega)|$ can have been caused by a broader MWD or the introduction of LCB. In this study, for the peroxide-modified LLDPE, the decrease could only be attributed to the introduction of LCB because the polydispersity remained approximately constant according to the SEC analysis (Figure 1).

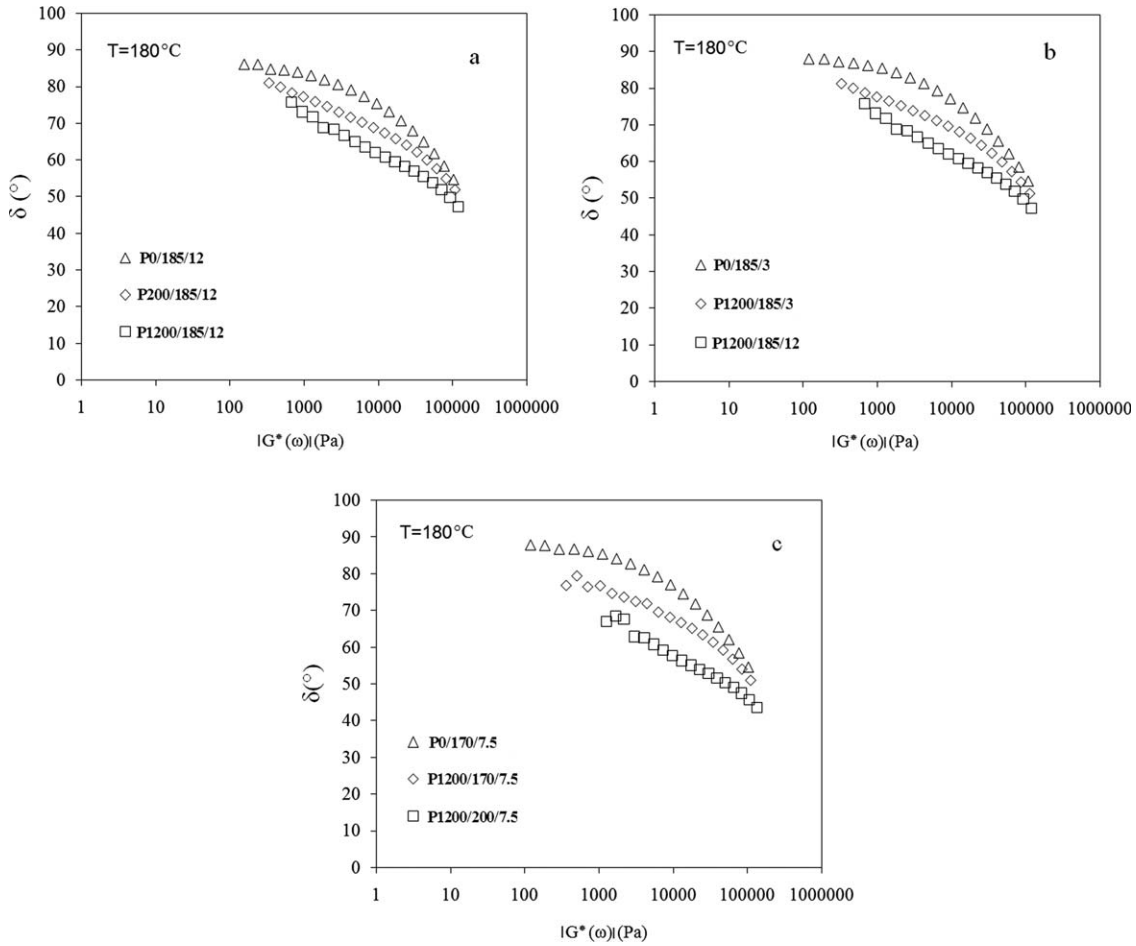

Figure 6. δ versus the processing conditions. The effects of the (a) peroxide concentration, (b) processing time, and (c) processing temperature.

Reaction Steps:

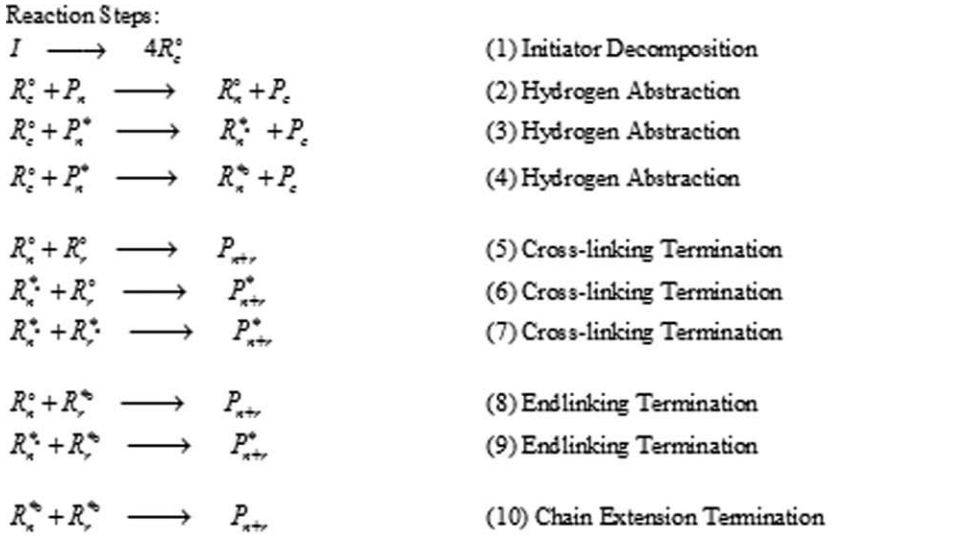

Description:

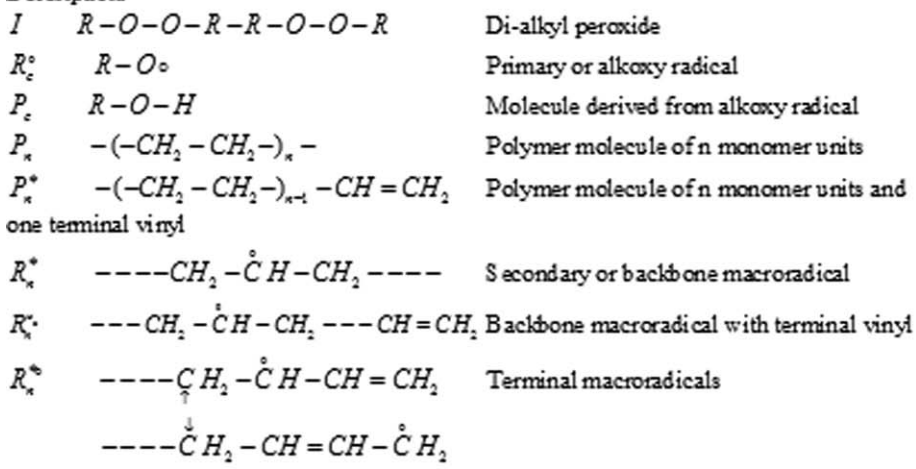

Product of Cross-linking Termination:

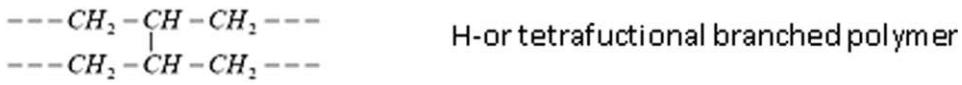

Product of Endlinking Termination:

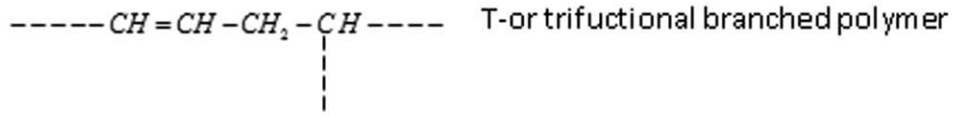

Product of Chain Extension Termination:

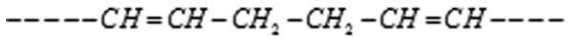

Scheme 1. Reactions of PE initiated by free radicals.[35]

Theory

Theoretical Estimation of *x*. Any attempt to correlate the evolving molecular architecture to rheology in the course of chemical modification first requires a consideration of the range of structural variation that the specific modifier may generate.[34] In the presence of free radicals, such as the decomposition products of peroxides, PE will undergo many different reactions (Scheme 1).[35]

Dominant chemical reactions include the initiator decomposition, radical attack of backbone hydrogen atoms, scission of the chains, and termination by combination. Three termination

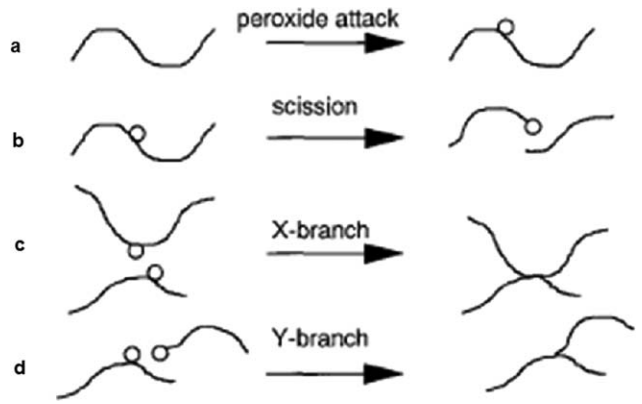

Scheme 2. Chemical reactions that modify the polymer molecular structure during simultaneous random scission and crosslinking.[42]

reactions that change the initial structure of PE are the crosslinking termination (tetrafunctional-branched polymer or X-branch formation), end-linking termination (trifunctional-branched polymer or Y-branch formation), and chain extension termination (Scheme 2).[35,42]

Correlating the rheological behavior with the microstructural evolution in a melt undergoing LCB reactive modification necessitates a number of simplifying assumptions concerning the extent, nature, and mechanism of the induced changes and the molecular size and architecture of the end product. Regardless of whether this modification occurs accidentally due to degradation or is caused deliberately to improve the processability, the following points are known:[31]

1. Linear polymer chains of initial (weight-average) molecular mass (M_L) break through scission, and some of their fragments crosslink with neighbors to form new molecules.
2. Of those newly created units, the ones resulting from fragments connected close to a chain-end maintain, more or less, the linear architecture of their precursors, whereas the rest assume branched configurations.
3. If the modification is of limited extent and does not progress much above the insertion of a single branching point per molecule on average, the following is also expected:
4. Most of the reacted linear fragments end up as parts of larger branched polymers. A fraction of the initially linear chains, with an average molecular mass M_L, after breaking (on the average) in the middle, crosslinks with mostly unbroken chains.[31]

If termination does not occur too far from a chain middle point, this results in structures resembling three-armed stars of average arm molecular mass [$M_a \approx M_L/2$; Scheme 2(d)] and, therefore, total molecular mass ($M_B = 3M_a \approx 3M_L/2$; trifunctional-branched polymer or Y-branch formation). If a termination reaction occurs between two backbone macroradicals [Scheme 2(c)], this results in structures resembling tetra-armed stars of $M_a \approx M_L/2$ and, therefore, $M_B = 4M_a \approx 2M_L$ (tetrafunctional-branched polymer or X-branch formation). If such an addition occurs close to a free end or if it pertains to a small fragment, it merely affects the linear chain population.

Hence, during reactive modification, we are dealing with a star linear (SL) polymer blend of newly formed L_2 (linear-to-linear chain transformations), S_3 (trifunctional-branched polymer or Y-branch formation), and S_4 (tetrafunctional-branched polymer or X-branch formation) molecules coexisting with unreacted L_1 precursors. The pertinent concentrations of the four structural variations are Φ_{Li} and Φ_{Sj}, where i is equal to 1 or 2, and j is the number of arms and is equal to 3 or 4.

An estimate for Φ_{Sj} may be obtained if one theorizes that a peroxide reaction with an L_1 chain is a statistically independent phenomenon and that the number of polyadditions exceeding four original L_1's is insignificant. Therefore, the diminishing probability of j chains to join on a single site [prob(j)] is equal to prob$(2)^{j-1}$, where prob indicates the probability. Then, the constituents of the SL melt are as follows:

- A $\phi_{L2} = \phi_2$ fraction of linear chains with $M_w \approx M_{L1}$.
- A $\phi_{S3} = {\phi_2}^2$ fraction of three-armed stars, with $M_a \approx M_L/2$ and, thus, total $M_w \approx 3M_L/2$
- A $\phi_{S4} = {\phi_2}^3$ fraction of four-armed stars, with $M_a \approx M_L/2$ and, thus, total $M_w \approx 2M_{L1}$
- A $\phi_{L1} = 1 - \phi_2 - {\phi_2}^2 - {\phi_2}^3$ fraction of unreacted original linear chains of $M_w = M_{L1}$.

Therefore, at any instant of the reactive process progression, the melt under modification may be considered as a mixture of

1. A $\phi_L = 1 - {\phi_2}^2 - {\phi_2}^3$ fraction of linear polymers, with $M_L \approx M_{L1}$.
2. A $\phi_S = {\phi_2}^2 + {\phi_2}^3$ fraction of three- and four-armed star polymers, in which M_w of each arm is equal to $M_a \approx M_L/2$.

With regard to η_0 of a linear chain melt, it is known that it depends on M_L according to the following approximate power law:[10,43,44]

$$\eta_L \approx \eta_C \left(\frac{M_L}{M_C}\right)^{3.5} \tag{5}$$

where M_C is the minimum M_L required for entanglements to start forming; it is a material constant that depends on the molecular rigidity of the polymer and, therefore, is affected by its chemical microstructure (Table 2.7 in ref. 43). It has been observed that M_C is equal to twice the molecular weight between two successive entanglements ($M_C \approx 2M_e$). For PE, $M_C = 3000$ g/mol. M_C is independent of branching when the presence of gel is too minute, as in this case.[45] η_C is the melt viscosity at the entanglement crossover, that is, where $M_L = M_C$, and at the given temperature. The viscosity of the three- and four-armed star polymers (η_S), varies exponentially with the molecular weight of each of their tethered arms:[46–48]

$$\eta_L \approx \eta_C \exp\left\{\alpha\left(\frac{M_a}{M_e} - 1\right)\right\} \tag{6}$$

where $M_a \approx M_{L1}/2$ and the coefficient α is independent of the branching point f for small fs.[47] According to molecular theory, the coefficient α is independent of the branching point f and is equal to 15/8. A comparison with experiments indicated a smaller value instead ($\alpha = 0.43$–0.6).[31]

Table IV. Comparison of x Values Calculated with Eqs. (9) and (10) According to Jorgenson et al.[20]

Sample code	[1,3-BDSA] (ppm)	η_0 (kPa s)	β_W (branch points/ molecule)	β_W[a]	β_W[b]
1	0	2.4 ± 0.05			
2	16	2.4 ± 0.05			
3	128	2.8 ± 0.1	0.063	0.014	0.016
4	257	3.4 ± 0.1	0.080	0.031	0.043
5	512	6.3 ± 0.2	0.120	0.087	0.102
6	1027	45 ± 3.0	0.240	0.263	0.309

[a] Calculated with eq. (10).
[b] Calculated with eq. (9).

Implicit to eq. (6) is the assumption that $\eta_S(M_a = M_e) \approx \eta_C \equiv \eta_L(M_C)$. In other words, it is stipulated that a star polymer of $M_a = M_e$ and a linear chain (which is in essence a two-armed star) of the same arm length ($M_L/2 = M_e$) have roughly the same viscosity. This is physically reasonable and has been proven helpful in circumventing the lack of available η_S data at the entanglement threshold.[31]

Phenomenology, corroborated by dynamic dilution theory,[49–51] dictates that the viscosity of an SL polymer blend (η_{SL}) is the logarithmic sum of the viscosities of its S and L components; that is, $\eta_{SL} \approx (\eta_S)^{\phi S}(\eta_L)^{1-\phi S}$. The viscosity of the melt under reactive modification is, therefore, equivalent to

$$\eta_{SL} \approx \eta_C \exp\left\{\alpha\phi_s\left(\frac{M_{L1}}{M_C}-1\right)\right\}\left(\frac{M_L}{M_C}\right)^{3.5(1-\phi_S)} \quad (7)$$

By incorporating the rational thoughts previously discussed, with regard to the ϕ_{Li} and ϕ_{Sj} variation, eq. (7) may be restated as follows:

$$\eta_{SL} \approx \eta_C \exp\left\{\alpha\left(\phi_2^2+\phi_2^3\right)\left(\frac{M_{L1}}{M_C}-1\right)\right\}\left(\frac{M_{L1}}{M_C}\right)^{3.5\left(1-\phi_2^2-\phi_2^3\right)} \quad (8)$$

Finally, by taking into consideration that $M_{L1} \approx M_C(\eta_{L1}/\eta_C)^{1/3.5}$, eq. (8) may also be expressed, more conveniently, in terms of the viscosity of the precursor melt (η_{L1}):

$$\eta_{SL} \approx \eta_C \exp\left\{\alpha\left(\phi_2^2+\phi_2^3\right)\left(\left[\frac{\eta_{L1}}{\eta_C}\right]^{1/3.5}-1\right)\right\}\left(\frac{\eta_{L1}}{\eta_C}\right)^{\left(1-\phi_2^2-\phi_2^3\right)} \quad (9)$$

From this equation, ϕ_2 can be determined. Because this equation is nonlinear, with the help of a numerical analysis method with MATLAB software, the ϕ_2 values can be obtained. With the ϕ_2 data, the ϕ_{S3} and ϕ_{S4} values can be calculated, and according to LCB = $\phi_{s3} + \phi_{s4}$, x can be determined.

Experimental Data versus Theoretical Data. Tsenoglou and coworkers[31,32] performed studies similar to this one. Their work considered the light crosslinking of PP and its consequences on the rheological properties. They developed a theory relating η_0 to x.[31] The theory assumes that for low levels of crosslinking, the polymer material consists of a fraction of linear chains and a fraction x of stars with an arm length half of the average length of the linear precursor. It is easy to show that under these assumptions, x equals the weight-average number of branch points per molecule (β_W). The theory of Tsenoglou and coworkers is expressed through the following equation:

$$\beta_W = \frac{\ln\left\{\frac{\eta_0^{BL}}{\eta_0}\right\}}{\alpha\left[\left(\frac{M_L}{M_C}\right)-1\right]-3\ln\left\{\frac{M_L}{M_C}\right\}} \quad (10)$$

where $\eta_0^{BL}<$ and η_0 are the zero-shear viscosities of the linear–star blend and the linear precursor, respectively, and α is a constant. Molecular theory predicts that $\alpha = 15/8$, but the experiments suggest that $\alpha = 0.4$–0.6.[31] M_L is the molecular weight of the linear precursor, and M_C is the critical entanglement molecular weight. Tsenoglou and coworkers[31,32] found a good correlation of SEC and rheometry results through eq. (10).

To compare the x values calculated by eq. (9) with those obtained in this study for the peroxide-modified PE and x values calculated by eq. (10), the data from Jørgensen et al.'s[20] work was used. Jørgensen used a metallocene synthesized high-density PE with a M_w of 82,000 and a number-average molecular weight of 40,000 g/mol modified with small amounts of 1,3-benzenedisulfonyl azide (1,3-BDSA) by reactive extrusion at 200°C with the purpose of forming long-chain branches. Equation (10) was developed on the basis of three-armed branch

Table V. η_0 Values for Each of the Molecular Architectures Present in the Peroxide-Modified LLDPE

Sample code: ppm/°C/min	η0 (Pa s)			
	160°C	180°C	190°C	200°C
P200/170/7.5	4,500	3,205	2,730	2,346
P200/185/3	5,301	3,894	3,435	3,115
P200/185/12	10,262	8,009	7,198	6,572
P200/200/7.5	10,657	8,764	8,027	7,490
P700/170/3	9,767	7,350	6,580	6,077
P700/170/12	8,077	7,791	6,619	6,764
P700/185/7.5	12,770	10,355	9,594	9,191
P700/200/3	12,276	9,981	8,709	7,333
P700/200/12	23,103	16,676	15,643	14,591
P1200/170/7.5	10,975	9,505	8,784	8,000
P1200/185/3	10,545	7,872	7,149	6,885
P1200/185/12	24,298	17,443	15,483	13,504
P1200/200/7.5	48,949	36,850	31,200	25,094
P0/170/3	—	3,121	—	—
P0/170/7.5	—	3,185	—	—
P0/170/12	—	3,210	—	—
P0/185/3	—	3,115	—	—
P0/185/7.5	—	3,298	—	—
P0/185/12	—	3,348	—	—
P0/200/3	4,554	3,733	3,391	3,049
P0/200/7.5	5,724	4,809	4,420	4,031
P0/200/12	9,643	7,667	6,747	5,828
P0/0/0	4,506	3,261	2,707	2,153

Table VI. Predicted Volume Fractions and x Values for Each of the Molecular Architectures Present in the Peroxide-Modified LLDPE as Functions of the Modifier Concentration, Mixing Time, and Mixing Temperature Used in the Reactive Modification According to Eq. (9)

Sample Code: ppm/°C/min	x	Volume fraction			
		Φ_{L1}	Φ_{L2}	Φ_{S3}	Φ_{S4}
P200/170/7.5	0.0006	0.9740	0.0250	0.0006	0.0000
P200/185/3	0.0183	0.8543	0.1274	0.0162	0.0021
P200/185/12	0.0751	0.6793	0.2456	0.0603	0.0148
P200/200/7.5	0.0835	0.6588	0.2577	0.0664	0.0171
P700/170/3	0.0683	0.6967	0.2351	0.0553	0.0130
P700/170/12	0.0687	0.6955	0.2358	0.0556	0.0131
P700/185/7.5	0.0972	0.6267	0.2760	0.0762	0.0210
P700/200/3	0.0898	0.6440	0.2663	0.0709	0.0189
P700/200/12	0.1348	0.5456	0.3196	0.1021	0.0326
P1200/170/7.5	0.0904	0.6424	0.2671	0.0714	0.0191
P1200/185/3	0.0746	0.6806	0.2448	0.0599	0.0147
P1200/185/12	0.1340	0.5472	0.3188	0.1016	0.0324
P1200/200/7.5	0.1878	0.4419	0.3702	0.1371	0.0507
P0/170/3	—	—	—	—	—
P0/170/7.5	—	—	—	—	—
P0/170/12	—	—	—	—	—
P0/185/3	—	—	—	—	—
P0/185/7.5	—	—	—	—	—
P0/185/12	—	—	—	—	—
P0/200/3	0.0173	0.8583	0.1241	0.0154	0.0019
P0/200/7.5	0.0377	0.7835	0.1788	0.0320	0.0057
P0/200/12	0.0702	0.6918	0.2381	0.0567	0.0135
P0/0/0	0	1	0	0	0

structures whereas, eq. (9) considers both three-armed and four-armed mechanisms. The obtained results in terms of the β_W values are summarized in Table IV. The purpose of the presented comparison between the two equations is to show which mechanism is more close to the real situation. The performed comparison indicated that the results obtained from eq. (9) were in better agreement with the experimental results; this implied that the creation of three-armed and four-armed branch structures are more probable in the peroxide modification process. Because Jørgensen et al. used β_W, here, the same terminology is also used. Actually, β_W is equal to α. Table V shows the η_0 data that was obtained from the linear viscoelastic measurements.

The P0 series of samples was prepared to determine whether the applied processing conditions affected the structure of LLDPE in the absence of peroxide or not. The results indicate

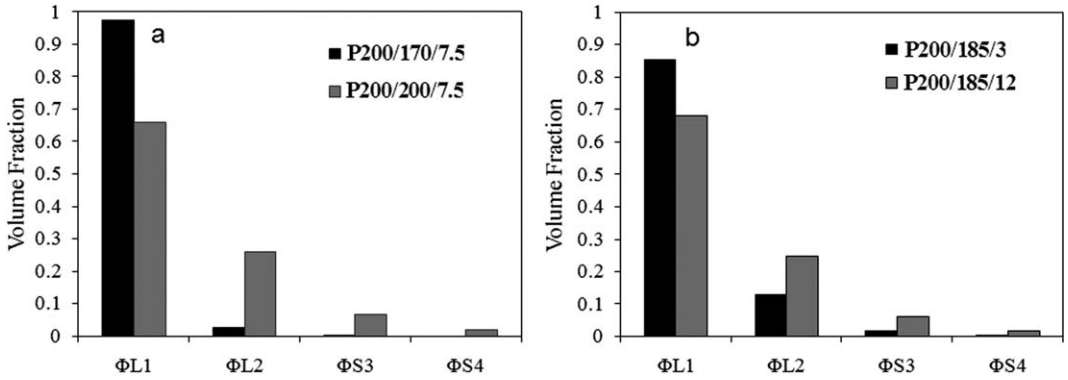

Figure 7. Volume fraction of each species of linear-branch samples. Effects of the (a) mixing temperature and (b) mixing time.

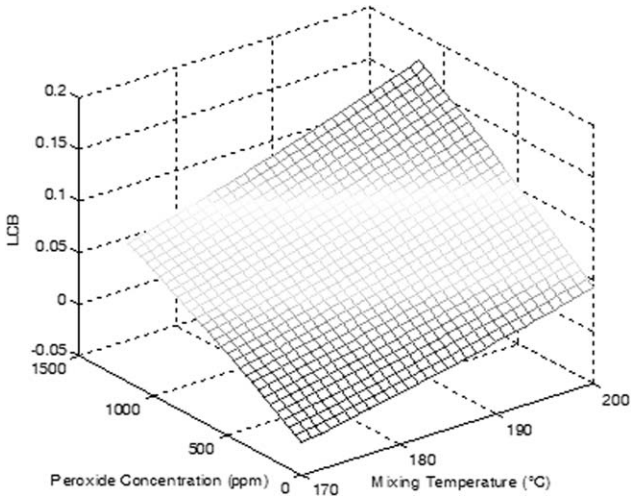

Figure 8. Relation between the peroxide concentration, mixing temperature, and x obtained by the model for the LLDPE melt-mixed for 7.5 min.

that there were no detectable changes in the rheological behavior of the samples prepared at low temperatures, that is, 170 and 185°C. This was evident when the η_0 data for the reference sample, that is, P0/0/0, were compared with that of the P0 series samples prepared at low temperatures (i.e., P0/170/3, P0/170/7.5, P0/170/12, P0/185/3, and P0/185/7.5). As shown from the data in Table V, the η_0 values for this P0 series of samples measured at 180°C were in the range 3100–3300 Pa s. This was very close to η_0 of the reference sample, which was about 3261 Pa s. However, those samples prepared at 200°C (i.e., the P0/200 series) showed some obvious changes in the η_0 values as compared to the reference sample. This change in the rheological behavior was attributed to structural changes induced by the presence of LCB. The structural changes induced in the absence of peroxide were attributed to a phenomenon known as *thermal modification,* which has been reported by other researchers as well.[52] Under these conditions, the branching was initiated by the two simultaneous factors high heat and shearing. Considering the mechanism proposed for this phenomenon transfer, the scission and termination reactions were similar to a peroxide modification reaction. In peroxide modification, the primary radical comes from the thermal decomposition of peroxide, whereas the initial source of radical formation in thermal degradation is based on chain scission and hydrogen abstraction. η_0 of the P700/170/3 sample at 160°C was slightly higher than that of P700/170/12, despite its lower peroxide concentration. This might have been due to the fact that the sample showed more non-Newtonian behavior at lower temperatures, and therefore, it might not have showed a proper Newtonian plateau. This caused the error in the determination of η_0 data for the P700/170/3 sample at 160°C. At higher temperatures, namely, 180 or 200°C, such behavior was not observed because of shifts toward more Newtonian behavior.

The η_0 data at 190°C were fed into eq. (9), and x and the volume fraction of each species of linear-branch samples were calculated. Table VI shows the predicted volume fractions and x values for each of the molecular architectures present in the peroxide-modified LLDPE as a function of the modifier concentration, mixing time, and mixing temperature used in the reactive modification according to eq. (9).

Figure 7(a,b) shows the effect of the mixing temperature and mixing time on the volume fraction of each species of linear-branch samples (P200/170/7.5, P200/200/7.5 and P200/185/3, and P200/185/12), including the unreacted original linear fraction (ϕ_{L1}), linear fraction (ϕ_{L2}), three-armed-star fraction (ϕ_{S3}), and four-armed-star fraction (ϕ_{S4}). As shown, the increase in the reaction temperature resulted in an increase in LCB. By knowing this prediction, we could predict the LCB value under different process conditions, such as time and temperature, before the reactive modification was performed in the extruder. This point is important from an industrial point of view because these parameters have a direct influence on the properties and performance of modified LLDPE.

As mentioned before, the mixing time and temperature affected the peroxide modification process enormously. When these parameters were increased, the volume fraction of the branch species increased rapidly. x had an efficient value. Any positive or negative deviation from this value resulted in a failure of the desirable properties of the modified samples. Therefore, knowing the efficient process parameters, including the mixing time and temperatures, made it easy to reach the expected LCB. The combined effects of the time and temperature of melt mixing and the peroxide concentration on x could best be illustrated through the three-dimensional plots presented in Figures 8 and 9. From these figures, one can obtain LCB by adjusting the other factors. Therefore, these three-dimensional diagrams show the importance of the simple rheological model in predicting the efficient process conditions.

CONCLUSIONS

Long-chain branches can be introduced into linear PE by peroxide modification, without gel formation. It was found that with an increase in the peroxide level, an increase in the number of

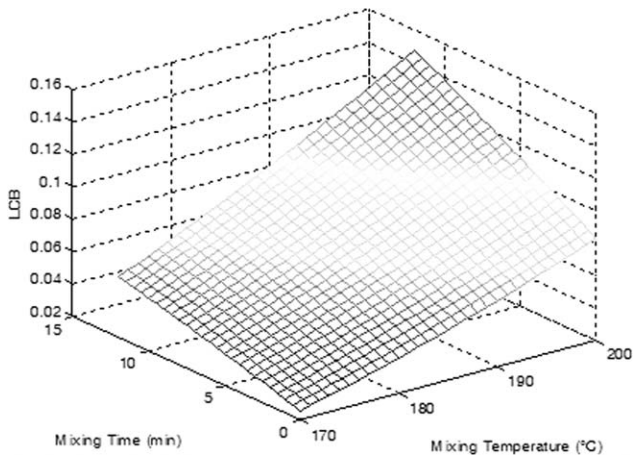

Figure 9. Relation between the mixing time, mixing temperature, and x obtained by the model for the LLDPE melt-mixed with 700 ppm peroxide.

long-chain branches occurred. From oscillatory shear flow measurements, a deviation of the δ–$|G^*|$ curve from that of the linear LLDPE was found; this was attributed to the presence of LCB. A significant increase in the η_0 values of the modified samples compared to those of the unreacted LLDPE of the same M_w was observed. This increase was explained by the small amount of LCB with relatively long arms and, hence, a high ratio of M_a to M_e, which had an exponential influence on η_0. Good agreement between the experimental and theoretical results was found; this showed that the rheological method was able to predict the processing conditions. Therefore, this method could potentially be used to investigate the effect of process parameters such as the mixing time, mixing temperature, and peroxide concentration versus x.

ACKNOWLEDGMENTS

One of the authors (H.A.K.) thanks the Alexander von Humboldt Foundation for its financial support. Also, technical assistance from A. Lederer and B. Kretzschmar is deeply appreciated.

REFERENCES

1. Graessley, W. W. *Acc. Chem. Res.* **1977**, *10*, 332.
2. Chen, X.; Costeux, C.; Larson, R. G. *J. Rheol.* **2010**, *54*, 1185.
3. McLeish, T. C. B.; Milner, S. T. *Adv. Polym. Sci.* **1999**, *143*, 195.
4. Wood-Adams, P.; Dealy, J. M. *Macromolecules* **2000**, *33*, 7481.
5. Klimke, K.; Parkinson, M.; Piel, C.; Kaminsky, W.; Spiess, H. W.; Wilhelm, M. *Macromol. Chem. Phys.* **2006**, *207*, 382.
6. Stadler, F. J.; Piel, C.; Klimke, K.; Kaschta, J.; Parkinson, M.; Wilhelm, M.; Kaminsky, W.; Münstedt, H. *Macromolecules* **2006**, *39*, 1474.
7. Agarwal, R.; Horsk, J.; Stejskal, J.; Quadrat, O.; Kratochvil, P. *J. Appl. Polym. Sci.* **1983**, *28*, 3453.
8. Malmberg, A.; Gabriel, C.; Steffl, T.; Münstedt, H.; Lofgren, B. *Macromolecules* **2002**, *35*, 1038.
9. Tackx, P.; Tacx, J. C. J. F. *Polymer* **1998**, *39*, 3109.
10. Zimm, B. H.; Stockmayer, W. H. *J. Chem. Phys.* **1949**, *17*, 1301.
11. Crosby, B. J.; Mangnus, M.; de Groot, W.; Daniels, R.; McLeish, T. C. B. *J. Rheol.* **2002**, *46*, 401.
12. Gabriel, C.; Münstedt, H. *Rheol. Acta* **1999**, *38*, 393.
13. Gabriel, C.; Münstedt, H. *Rheol. Acta* **2002**, *41*, 232.
14. Gabriel, C.; Münstedt, H. *J. Rheol.* **2003**, *47*, 619.
15. Golriz, M.; Khonakdar, H. A.; Morshedian, J.; Jafari, S. H.; Mohammadi, Y.; Wagenknecht, U. *Macromol. Theory Simul.* **2013**, DOI: 10.1002/mats.201300118.
16. Dordinejad, A. K.; Jafari, S. H. *Polym. Eng. Sci.* **2013**, DOI: 10.1002/pen.23652.
17. Vega, J. F.; Santamaria, A.; Munoz-Escalona, A.; Lafuente, P. *Macromolecules* **1998**, *31*, 3639.
18. Wood-Adams, P. M.; Dealy, J. M.; de Groot, A. W.; Redwine, O. D. *Macromolecules* **2000**, *33*, 7489.
19. Wood-Adams, P. M.; Costeux, S. *Macromolecules* **2001**, *34*, 6281.
20. Jorgensen, J. K.; Stori, A.; Redford, K.; Ommundsen, E. *Polymer* **2005**, *46*, 12256.
21. Tasanatanachai, P.; Tzoganakis, C.; Magaraphan, R. *Int. Polym. Proc.* **2008**, *2*, 168.
22. Passaglia, E.; Coiai, S.; Giordani, G.; Taburoni, E.; Fambri, L.; Pagani, V.; Penco, M. *Macromol. Mater. Eng.* **2004**, *289*, 809.
23. Dordinejad, A. K.; Jafari, S. H.; Khonakdar, H. A.; Wagenknecht, U.; Heinrich, G. *J. Appl. Polym. Sci.* **2013**, *129*, 458.
24. Dordinejad, A. K.; Jafari, S. H. *J. Appl. Polym. Sci.* **2013**, DOI:10.1002/app.39560.
25. Stadler, F. J.; Nishioka, A.; Stange, J.; Koyama, K.; Münstedt, H. *Rheol. Acta* **2007**, *46*, 1003.
26. Stadler, F. J.; Gabriel, C.; Münstedt, H. *Macromol. Chem. Phys.* **2007**, *208*, 2449.
27. Dealy, J. M.; Larson, R. G. Structure and Rheology of Molten Polymers from Structure to Flow Behavior and Back Again; Hanser: Munich, **2006**.
28. Stadler, F. J. *Rheol. Acta* **2012**, *51*, 821.
29. Berry, G. C.; Fox, T. G. *Adv. Polym. Sci.* **1968**, *5*, 261.
30. Ferry, J. D. Viscoelastic Properties of Polymers; Wiley: New York, **1980**.
31. Tsenoglou, C. J.; Gotsis, A. D. *Macromolecules* **2001**, *34*, 4685.
32. Tsenoglou, C. J.; Kiliaris, P.; Papaspyrides, C. D. *Macromol. Mater. Eng.* **2011**, *296*, 630.
33. Smedberg, A.; Hjertberg, T.; Gustafsson, B. *Polymer* **1997**, *38*, 4127.
34. Suwanda, D.; Balke, S. T. *Polym. Eng. Sci.* **1993**, *33*, 1585.
35. Suwanda, D.; Balke, S. T. *Polym. Eng. Sci.* **1993**, *33*, 1592.
36. Gustafsson, B.; Boström, J. O.; Dammert, R. C. *Macromol. Mater. Eng.* **1998**, *261*, 93.
37. Auhl, D.; Stange, J.; Munstedt, H.; Krause, B.; Voigt, D.; Lederer, A.; Lappan, U.; Lunkwitz, K. *Macromolecules* **2004**, *37*, 9465.
38. Sugimoto, M.; Tanaka, T.; Masubuchi, Y.; Takimoto, J.; Koyama, K. *J. Appl. Polym. Sci.* **1999**, *73*, 1493.
39. Golriz, M.; Khonakdar, H. A.; Morshedian, J.; Abedini, H.; Jafari, S. H.; Lederer, A.; Wagenknecht, U. *Macromol. Mater. Eng.*, **2013**, DOI:10.1002/mame.201300005.
40. Trinkle, S.; Walter, P.; Friedrich, C. *Rheol. Acta* **2002**, *41*, 103.
41. Stadler, F. J.; Münstedt, H. *Macromol. Mater. Eng.* **2009**, *294*, 25.
42. Gloor, P. E.; Tang, Y.; Kostanska, A. E.; Hamielec, A. E. *Polymer* **1994**, *35*, 1012.
43. Graessley, W. W. Polymeric Liquids and Networks: Dynamics and Rheology; Garland Science: New York, **2008**.
44. Pearson, D. S. *Rubber Chem. Technol.* **1987**, *60*, 439.

45. Fetters, L. J.; Lohsey, D. J.; Colby, R. H. In Physical Properties of Polymers Handbook; Mark, J. E., Ed.; Springer: New York, **2007**.
46. Doi, M.; Kuzuu, N. Y. *J. Polym. Sci. Polym. Lett. Ed.* **1980**, *18*, 775.
47. Pearson, D. S.; Helfand, E. *Macromolecules* **1984**, *17*, 888.
48. Kraus, G.; Gruver, J. T. *J. Polym. Sci.* **1965**, *3*, 105.
49. Struglinski, M. J.; Graessley, W. W.; Fetters, L. *J. Macromolecules* **1988**, *21*, 783.
50. Ball, R. C.; McLeish, T. C. B. *Macromolecules* **1989**, *22*, 1911.
51. Blottiere, B.; McLeish, T. C. B.; Hakiki, A.; Young, R. N.; Milner, S. T. *Macromolecules* **1998**, *31*, 9295.
52. Epacher, E.; Fekete, E.; Gahleitner, M.; Pukanszky, B. *Polym. Degrad. Stab.* **1999**, *63*, 489.